Measuring Ejecta Velocities in Tycho's and Kepler's Supernova Remnants with the *Chandra* HETGS

M. Millard[1], J. Bhalerao[1], S. Park[1], T. Sato[2], J. P. Hughes[3], P. Slane[4], D. Patnaude[4], D. Burrows[5], and C. Badenes[6]

[1]University of Texas at Arlington, [2]RIKEN, [3]Rutgers University, [4]Harvard-Smithsonian CfA, [5]Penn State Univ.,[6]University of Pittsburgh

The University of Texas ARLINGTON

ABSTRACT

We report measurements of the bulk radial velocity from a sample of small, X-ray emitting metal-rich ejecta knots in Kepler's and Tycho's supernova remnants (SNRs). We measure the Doppler shift of the He-like Si K line center energy in the spectra of these knots from our *Chandra* High-Energy Transmission Grating Spectrometer (HETGS) observations to estimate their radial velocities (v_r). Our preliminary results on the analysis of Tycho's SNR show radial velocities up to $v_r \sim 5{,}000$ km s^{-1} in ejecta knots near the center of the SNR. In Kepler's SNR, we estimate high radial velocities of up to $v_r \sim 8{,}000$ km s^{-1}. We also measure proper motions for these ejecta knots based on the archival Advanced CCD Imaging Spectrometer (ACIS) data of Kepler's SNR taken in 2000, 2006, and 2014. The fastest moving knots showed proper motions of up to ~ 0.2 arcseconds per year. A few knots with the highest radial velocities also exhibit large proper motions, indicating that they are nearly freely expanding. Assuming that these high velocity ejecta knots are freely expanding near or beyond the main SNR shell, we estimate a distance to Kepler of d ~ 4.8 to 8.2 kpc. The ejecta knots in our sample have an average space velocity of $v_s \sim 4{,}600$ km s^{-1} (at a distance of 6 kpc) in Kepler's SNR. We note that 8 out of the 15 ejecta knots from our sample show a statistically significant (at the 90% confidence level) redshifted spectrum, compared to only 2 with a blueshifted spectrum, suggesting an asymmetry in the ejecta distribution in Kepler's SNR along the line of sight. This work has been supported in part by NASA *Chandra* Grants GO6-17060X, GO7-18061X, and AR7-18006X.

Introduction

- Recent theoretical (e.g., Kasen et al. (2009)) and observational evidence (e.g., Maeda et al. (2010, 2011)) has shown that Type Ia supernova explosions may be asymmetrical events. An explosion asymmetry would in turn lead to an asymmetrical ejecta distribution in the resulting supernova remnant (SNR).
- A straightforward way to reveal the 3-D structure of ejecta is to measure the Doppler shifts in the emission lines from the X-ray-emitting ejecta knots projected over the face of their face, and thus their bulk motion v_r along the line of sight.
- We use our recent *Chandra* HETGS observations of two Type Ia remnants, Kepler's SNR and Tycho's SNR, (Figure 1) to make precise v_r measurements of small ejecta regions within each remnant. We also measure the proper motion (PM) of these regions using archival *Chandra* ACIS data. Based on these v_r and PM measurements, we aim to construct the 3-D ejecta structure in these SNRs.

Observations

- We performed our *Chandra* HETGS observation of Kepler using the ACIS-S array from 2016 July 20 to 2016 July 23. The observation is composed of a single ObsID, 17901, with a total effective exposure of 147.6 ks after reprocessing (see Figure 1).
- Our *Chandra* HETGS (ACIS-S) observation of Tycho was performed from 2017 October 17 to 2017 November 19 and is composed of 13 ObsIDs, with a total effective exposure of 442.3 ks (see Figure 1).
- We also used archival *Chandra* ACIS data of Kepler from 2000, 2006, and 2014 (~ 930 ks total exposure) and Tycho from 2003, 2009, and 2015 (~ 1.17 Ms total exposure) as supplementary data to make spectral fitting and proper motion measurements.

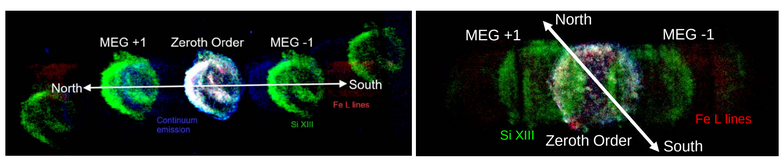

Figure 1. *Chandra* HETG 3-color image of Kepler's SNR (Left) and Tycho's SNR (Right). Red: 0.7-1.2 keV, Green: 1.7-2.0 keV and Blue: 2.0-8.0 keV. The Fe L complex and continuum emission appear smeared across the ACIS-S chips, the former because it consists of many emission lines, and the latter because it lacks individual emission lines. The Si XIII (He-like Si K) emission is more focused on the detector, because it consists only of three closely spaced lines at 1.865 keV.

Kepler's Supernova Remnant

- A well-known Type Ia SNR interacting with circumstellar material (CSM) is the remnant of Supernova (SN) 1604, or Kepler's SNR (Kepler, hereafter), the most recent Galactic historical supernova.
- Young, ejecta-dominated remnant of a luminous (assuming a distance > 7 kpc) Type Ia SN (Patnaude et al. 2012) from a metal-rich progenitor (Park et al. 2013);
- Excellent opportunity to study the nature of a Type Ia progenitor and its explosion in the presence of CSM/nitrogen-rich gas (Dennefeld 1982; Blair et al. 1991; Burkey et al. 2013; Katsuda et al.2015).
- Distance to Kepler is not well constrained: ~ 3.9 (Sankrit et al. 2005) to > 7 kpc (Patnaude et al. 2012; Chiotellis et al. 2012).

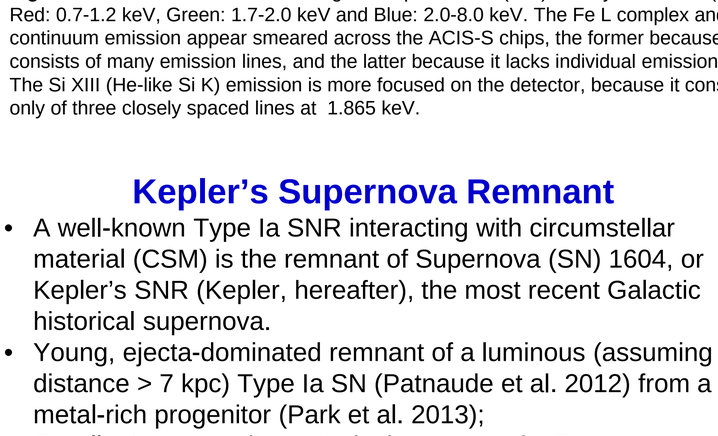

Figure 2. ACIS-S gray-scale image of Kepler's SNR from the 2014 observation, filtered to the energy range 1.7 to 2.0 keV. Seventeen ejecta and CSM knots which we analyzed in this work are marked with circles. CSM knots are marked with squares (also, their region names include " * "). Otherwise, we identify all other knots to be metal-rich ejecta based on our spectral analysis of the archival ACIS data. Cyan and red markers indicate blue- and red-shifted features, respectively, while green represents statistically negligible v_r at the 90% confidence interval. The numeric values are based on the descending order of the magnitudes of the estimated v_r: i.e., R1 shows the most redshifted spectrum and B1 the most blueshifted. The uncertainty in the kinematic center of the SNR estimated by Sato & Hughes (2017b) is denoted by a dotted yellow circle. A zoomed-in image of knot R1 is shown in the upper left corner.

Analysis

- Our primary goal is to measure the atomic line center energies in the X-ray emission spectrum for small individual emission features within an SNR using the bright line triplet, He-like Si K.
- The utility of the HETG spectrum is affected when the source is extended and/or surrounded by complex background emission features, e.g. supernova remnants.
- We selected features which generally satisfy the selection criteria determined from our ray-trace simulations of *Chandra* observations (see Millard et al. (2019)) and are bright in the He-like Si K band (1.7 – 2.0 keV).
- For each extracted region, the line center energies of the He-like Si K triplets were measured with gaussian models (Figure 3).
- We compared the measured line center wavelengths with the rest values to measure the Doppler shifts in these lines, and thus to estimate the corresponding v_r.
- We also measure proper motions (μ) based on archival *Chandra* data in Kepler for each knot.

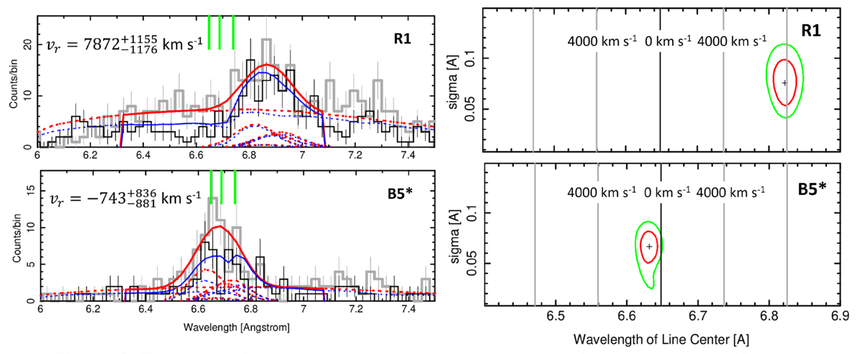

Figure 3. Examples of our line center energy measurements for small emission features in Kepler. The left column is the HETG spectra overlaid with the best fit model. The right column shows the confidence level contours for the best fit v_r value. Regions R1 shows a clearly redshifted spectra. Region B5* shows negligible Doppler shift. The green lines show the locations of the rest frame He-like Si K triplet line center wavelengths. The dashed lines show individual Gaussian components of our best fit model. The errors represent a 90% confidence interval. Gray: MEG +1 data, Black: MEG -1 data, Red: MEG +1 model fit, Blue: MEG -1 model fit.

Kepler Results and Discussion

- We measured the radial velocities and proper motions of 17 small emission features (15 ejecta and 2 CSM knots) in Kepler (Figure 2).
- We find a handful of knots are moving at speeds approaching 10^4 km s^{-1}, with expansion indices approaching 1, indicating nearly free expansion, generally consistent with the recent results based on the *Chandra* ACIS data (Sato & Hughes 2017b).
- Based on our radial velocity measurement of a fast-moving ejecta knot (R1), we estimate a distance to Kepler, *d* ~ 4.8 - 8.2 kpc.
- Most of our v_r measurements indicate a redshifted spectrum, suggesting an asymmetry in the along-the-line-of-sight ejecta distribution of the remnant (Figure 4).
- The results of our v_r and proper motion measurements are summarized in Table 1. We use these measurements to estimate the space velocity of each knot (for *d* = 6 kpc); we find an average space velocity of $v_s \sim 4{,}600$ km s^{-1} .

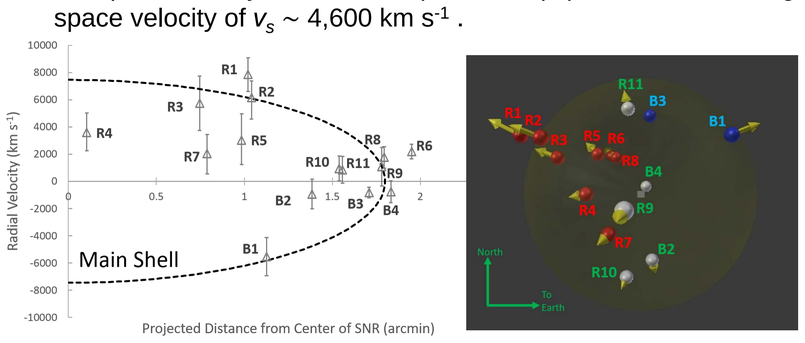

Figure 4. The left panel shows the positions of ejecta knots in vr vs. *r* (projected angular distance from the center of the SNR) space. The dashed line is the approximate location of the outermost boundary of the main SNR shell. The right panel shows a 3-D perspective of the locations of our measured ejecta knots. The red spheres represent redshifted knots, blue spheres are blueshifted knots, and white spheres are those with negligible Doppler shift. The gold arrows indicate the knots' relative magnitude of space velocities and directions. The shaded circle shows the approximate location of the main shell of Kepler's SNR.

Table 1. Radial Velocity and Proper Motions of Small Emission Features in Kepler's SNR

Region†	R.A.[a] (degree)	Dec[a] (degree)	D^b (arcmin)	v_r (km s^{-1})	$v_{r(SII)}$[c] (km s^{-1})	μ_{RA} (arcsec yr^{-1})	μ_{Dec} (arcsec yr^{-1})	μ_{Tot}[d] (arcsec yr^{-1})	η[e]	v_s[f] (km s^{-1})
R1(N2)	262.67314	−21.474812	1.02	7872^{+1155}_{-1176}	9110^{+30}_{-110}	0.028 ±0.017	0.137 ±0.024	0.140 ±0.029	0.94±0.14	8824^{+1073}_{-1091}
R2(N1)	262.68120	−21.476634	1.04	6165^{+1287}_{-1384}	8700^{+650}_{-470}	-0.065 ±0.016	0.081 ±0.024	0.104 ±0.028	0.68±0.10	6836^{+1189}_{-1274}
R3(N3)	262.66648	−21.480553	0.74	5745^{+2257}_{-2174}	5880^{+690}_{-1750}	0.045 ±0.016	0.078 ±0.024	0.090 ±0.028	0.83±0.16	6289^{+2077}_{-2002}
R4	262.67403	−21.491796	0.10	3589^{+1459}_{-1344}		0.019 ±0.018	-0.021 ±0.024	0.028 ±0.03	1.86±2.64	3679^{+1430}_{-1318}
R5	262.66124	−21.478912	0.98	3036^{+1857}_{-1668}		0.061 ±0.017	0.105 ±0.027	0.121 ±0.032	0.85±0.13	4600^{+1336}_{-1222}
R6	262.64087	−21.477378	1.95	2196^{+519}_{-524}		0.172 ±0.017	0.104 ±0.024	0.201 ±0.029	0.71± 0.05	6128^{+533}_{-534}
R7	262.67997	−21.502758	0.79	2052^{+1409}_{-1459}		-0.058 ±0.017	-0.064 ±0.024	0.086 ±0.029	0.75± 0.14	3203^{+1014}_{-1043}
R8	262.64352	−21.478218	1.79	1761^{+774}_{-748}		0.067 ±0.016	0.059 ±0.024	0.089 ±0.029	0.34± 0.03	3090^{+639}_{-629}
R9	262.70386	−21.495295	1.78	1074^{+1416}_{-920}		-0.171 ±0.016	-0.051 ±0.024	0.179 ±0.029	0.69± 0.06	5196^{+552}_{-505}
R10	262.66758	−21.517109	1.54	940^{+904}_{-887}		-0.033 ±0.018	-0.070 ±0.024	0.077 ±0.03	0.34± 0.03	2390^{+700}_{-697}
R11	262.66920	−21.465973	1.56	840^{+952}_{-931}		0.002 ±0.018	0.141 ±0.024	0.141 ±0.03	0.62± 0.06	4090^{+700}_{-698}
B6*	262.67685	−21.497011	0.41	-372^{+649}_{-799}		-0.047 ±0.016	-0.013 ±0.024	0.049 ±0.028	0.83± 0.30	1446^{+490}_{-505}
B5*	262.66782	−21.489190	0.29	-743^{+836}_{-881}		0.004 ±0.015	0.004 ±0.023	0.006 ±0.028	0.14± 0.07	762^{+824}_{-868}
B4	262.63949	−21.488767	1.83	-760^{+1045}_{-1012}		0.140 ±0.016	0.018 ±0.024	0.141 ±0.03	0.53± 0.04	4088^{+505}_{-502}
B3(Ej1-2)	262.65918	−21.466017	1.71	-814^{+388}_{-403}	244^{+46}_{-10}	0.026 ±0.015	0.026 ±0.023	0.037 ±0.028	0.15±0.01	1322^{+498}_{-502}
B2	262.66207	−21.512892	1.38	-930^{+1056}_{-1066}		0.058 ±0.017	-0.120 ±0.024	0.133 ±0.029	0.66± 0.07	3911^{+672}_{-673}
B1	262.68243	−21.475636	1.13	-5544^{+1350}_{-1471}		-0.054 ±0.018	0.077 ±0.024	0.094 ±0.03	0.57± 0.07	6154^{+1247}_{-1353}

*CSM-dominated knot. †Knot labels in parentheses are those used by Sato & Hughes (2017b).

[a] Position in 2016 (J2000).

[b] Projected angular distance from kinematic center estimated by Sato & Hughes (2017b); R.A.(J2000) = 17h 30m 41s.321 and Declination(J2000) = -21° 29' 30''.51, with uncertainties of R:A: = 0.073' and Dec = 0.072', respectively.

[c] Values taken from Sato & Hughes (2017b). Errors represent a 68% confidence interval.

[d] $\sqrt{\mu^2_{R.A.} + \mu^2_{Dec}}$.

[e] Expansion index. [f] Estimated space velocity for a distance of 6 kpc.

Tycho's Supernova Remnant

- Tycho's SNR (Tycho, hereafter) is the remnant of SN 1572. Its historical light curve (Baade 1945; Ruiz-Lapuente 2004), light echo spectrum (Krause et al. 2008), and X-ray ejecta spectral analysis (Badenes et al. 2006) point to a Type Ia origin.
- Infrared data show an ambient density variation between northeast and southwest of the SNR (Williams et al. 2013); X-ray and radio measurements of shock proper motion showed that Tycho is expanding into a medium generally without a significant radial density gradient (Reynoso et al. 1999; Hughes 2000).
- Our deep *Chandra* HETG observation of Tycho provides a unique opportunity to resolve the ejecta structure of a normal Type Ia SN in unprecedented detail. We perform v_r and proper motion measurements of small ejecta regions in Tycho with the same methods used in the analysis of Kepler.

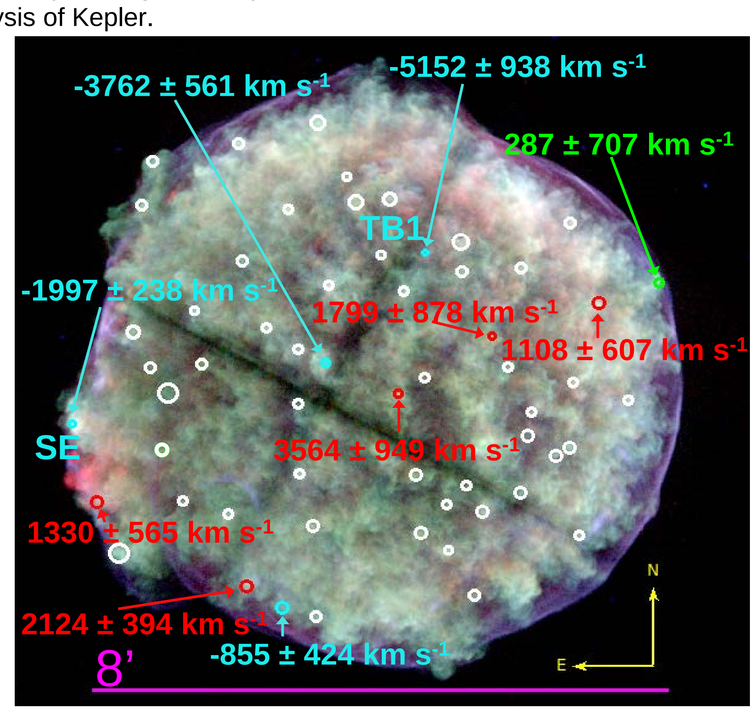

Figure 5. ACIS-I 3-color image of Tycho's SNR from the 2009 observation. Red: 0.7-1.2 keV, Green: 1.7-2.0 keV and Blue: 2.0-8.0 keV. Eleven ejecta knots which we analyzed in this work are marked with circles. Cyan and red markers indicate blue- and red-shifted features, respectively, while green represents statistically negligible v_r at the 90% confidence interval. The white circles indicate regions where we may make future v_r measurements.

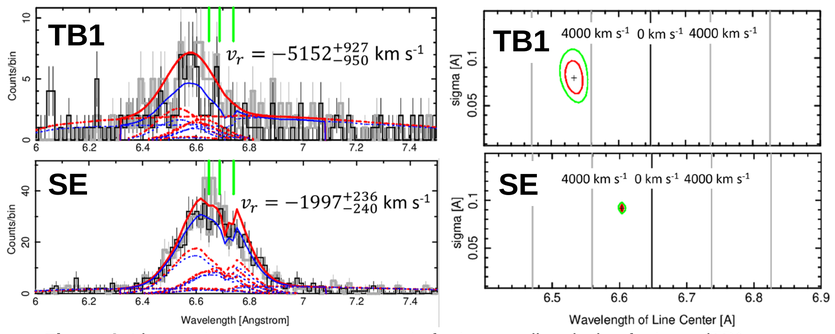

Figure 6. Line center energy measurements for two small emission features (TB1 and SE) in Tycho. The left column is the HETG spectra overlaid with the best fit model. The right column shows the confidence level contours for the best fit v_r value. Labels are the same as Figure 4.

Tycho Results and Discussion

- We have preliminarily measured the v_r of 10 ejecta knots in Tycho (Figure 5). We find radial velocities up to $v_r \sim 5{,}000$ km s^{-1}(Figure 6).
- Our v_r results are generally consistent with recent *Chandra* ACIS v_r measurements by Sato & Hughes (2017a) and Williams et al. (2017), in particular the high radial velocity ($v_r \sim$ -2,000 km s^{-1}) seen in the ejecta knot protruding beyond the southeastern outermost boundary.
- We find proper motions using archival *Chandra* ACIS data up to $\mu \sim 0.3$ arcseconds yr^{-1} (near the outer boundary) and $\mu \sim 0.14$ arcseconds yr^{-1} on average.
- Combining v_r and proper motion values gives space velocities up to $v_s \sim$ 6,000 km s^{-1} . The space velocity of the knots near the outer boundary is comparable to the knots near the center.

Future Work

- **A longer observation of Kepler using the *Chandra* HETGS** would be required to measure v_r for a significantly larger number of ejecta knots covering the entire face of the SNR (especially in the southern shell to test north-south asymmetry) to help construct a more complete picture of the 3-D distribution of ejecta, which is essential to provide observational constraints to establish more realistic Type Ia SN models.
- For our study of Tycho, we will continue to perform and refine our v_r and proper motion measurements of more ejecta knots (potentially ~ 50 regions) with the current data to study their spatial distribution throughout the entire SNR.

Acknowledgements

This work has been supported in part by NASA *Chandra* Grants GO6-17060X, GO7-18061X, and AR7-18006X. J.P.H. acknowledges support for supernova remnant research from NASA grant NNX15AK71G to Rutgers University. T.S. was supported by the Japan Society for the Promotion of Science (JSPS) KAKENHI Grant Number JP19K14739 and the Special Postdoctoral Researchers Program in RIKEN.

References

Baade, W. 1945, ApJ, 102, 309
Badenes, C. et al. 2006, ApJ, 645, 1373
Blair, W. P. et al. 1991, ApJ, 366, 484
Burkey, M. T., Reynolds, S. P., Borkowski, K. J., & Blondin, J. M. 2013, ApJ, 764, 63
Chiotellis, A. et al. 2012, A&A, 537, 139
Dennefeld, M. 1982, A&A, 112, 215
Hughes, J. 2000, ApJ, 545, L53
Kasen, D., Röpke, F. K., & Woosley, S. E. 2009, Nature, 460, 869
Katsuda S. et al. 2015, ApJ, 808, 49
Krause, O. et al. 2008, Nature, 456, 617
Maeda, K., Benetti, S., Stritzinger, M., et al. 2010, Nature,466, 82
Maeda, K., Leloudas, G., Taubenberger, S., et al. 2011, MNRAS, 413, 3075
Millard et al. 2019, ApJ, Submitted
Park, S. et al. 2013, ApJL, 767, L10
Patnaude, D. et al. 2012, ApJ, 756, 6
Reynoso, E. et al. 1999, AJ, 117, 1827
Ruiz-Lapuente, P. 2004, ApJ, 612, 357
Sato, T., & Hughes, J. P. 2017a, ApJ, 840, 112
Sato T., Hughes J. P., 2017b, ApJ, 845,167
Sankrit, R., Blair, W. P., Delaney, T., et al. 2005, Advances in Space Research, 35, 1027
Williams, B. et al. 2013, ApJ, 770, 129
Williams, B. J., Coyle, N. M., Yamaguchi, H., et al. 2017, ApJ, 842, 28